Available online at www.sciencedirect.com
SCIENCE DIRECT®
Clinical Biomechanics 20 (2005) 1038–1045
CLINICAL BIOMECHANICS
www.elsevier.com/locate/clinbiomech

The influence of static axial torque in combined loading on intervertebral joint failure mechanics using a porcine model

Janessa D.M. Drake, Crystal D. Aultman, Stuart M. McGill, Jack P. Callaghan *

Faculty of Applied Health Sciences, Department of Kinesiology, University of Waterloo, Waterloo, Ont., Canada N2L 3G1

Received 2 June 2004; accepted 14 June 2005

Abstract

Background. The spine is routinely subjected to repetitive combined loading, including axial torque. Repetitive flexion–extension motions with low magnitude compressive forces have been shown to be an effective mechanism for causing disc herniations. The addition of axial torque to the efficacy of failure mechanisms, such as disc herniation, need to be quantified. The purpose of this study was to determine the role of static axial torque on the failure mechanics of the intervertebral joint under repetitive combined loading.

Methods. Repetitive flexion–extension motions combined with 1472 N of compression were applied to two groups of nine porcine motion segments. Five N m of axial torque was applied to one group. Load–displacement behaviour was quantified, and planar radiography was used to document tracking of the nucleus pulposus and to identify fractures.

Findings. The occurrence of facet fractures was found to be higher ($P = 0.028$) in the axial torque group (7/9), compared to the no axial torque group (2/9). More hysteresis energy was lost up to 3000 cycles of loading in the axial torque group ($P < 0.014$). The flexion–extension cycle stiffness was not different between the two groups until 4000 cycles of loading, after which the axial torque group stiffness increased ($P = 0.016$). The percentage of specimens that herniated after 3000 cycles of loading was significantly larger ($P = 0.049$) for the axial torque group (71%) compared to the no axial torque group (29%).

Interpretation. Small magnitudes of static axial torque alter the failure mechanics of the intervertebral disc and vertebrae in combined loading situations. Axial torque appears to accelerate the susceptibility for injury to the intervertebral joint complex. This suggests tasks involving axial torque with other types of loading, apart from axial twist motion, should be monitored to assess exposure and injury risk.
© 2005 Elsevier Ltd. All rights reserved.

Keywords: Axial torque; Spine; Herniation; Injury; Cumulative loading

1. Introduction

Axial torques (AT) are experienced daily by the lumbar spine while performing domestic, athletic, and industrial tasks. Both axial rotation (Kelsey et al., 1984; Marras et al., 1993; Punnet et al., 1991) and cumulative compressive loading (Jager et al., 2000; Kumar, 1990; Norman et al., 1998) have been identified in epidemiologic studies as significant risk factors in developing low back injuries and/or pain. Damage to a facet joint (McCall et al., 1979; Schwarzer et al., 1994) or the intervertebral disc (IVD) (Ito et al., 1998; Boos et al., 2000) has the potential to cause low back pain. However, the onset of IVD injury/degeneration does not always coincide with onset of pain (Boden et al., 1990; Jensen et al., 1994), nor is there always diagnostic evidence to correlate damage with painful facet joints (Schwarzer et al., 1995b).

Several researchers have examined the partitioning of the AT resistance between the IVD and facets. Various

* Corresponding author.
E-mail address: callagha@healthy.uwaterloo.ca (J.P. Callaghan).

0268-0033/$ - see front matter © 2005 Elsevier Ltd. All rights reserved.
doi:10.1016/j.clinbiomech.2005.06.007

magnitudes of applied AT have been investigated: Farfan (1969) average maximum torque ranging from 23.7 to 32.7 N m, Krismer et al. (1996) ≈2–8.5 N m, Pearcy and Hindle (1991) between 12 and 25 N m, and Adams and Hutton (1981) 18–31.6 N m (with different grades of disc degeneration and varied compression between 377.8 and 624.5 N). Farfan (1969, 1970) concluded that AT damages the IVD prior to causing any bony damage. Krismer et al. (1996) reported that intact annulus fibres are more capable to restrict small axial torques than facet joints, and concluded AT is important in the development of disc degeneration. However, several researchers found that combined loading of AT and compression damages the facet joints and is not compromising to the structural integrity of the IVD (Adams and Hutton, 1981; Pearcy and Hindle, 1991). The opinion of these researchers was that intact facets protect the IVD from an AT load, so facet fracture must precede disc herniation. The potentially controversial findings regarding the role of AT in IVD failure mechanics are likely due to the use of different loading scenarios (i.e. with/without compression).

Risk factors identified for low back disorders in industry do not usually separate the effects of trunk AT from active trunk axial rotation; since these variables are inherently dependent (AT creates the rotation). Axial rotation has been reported to increase the risk of developing a low back disorder (i.e. herniation) when incorporated into lifting scenarios, or is a component of the required work posture (Kelsey et al., 1984; Marras et al., 1993; Punnet et al., 1991). Conversely, axial rotation was not associated with increased risk for developing a low back disorder when performed independent of lifting (Kelsey et al., 1984). The mechanism underlying the transformation of AT/axial rotation from benign to malignant when combined with other types of loading is unknown. Further, the structures involved in the failure resulting from combined loading with AT need to be identified. This is crucial information in the decision to create and implement guidelines governing the permissible repetitive exposure limit to AT, and to the diagnosis and subsequent treatment/rehabilitation assigned for the injuries.

Using porcine specimens, Callaghan and McGill (2001) demonstrated that herniation can be reliably created with modest levels of compression (867 N and 1472 N) with highly repetitive flexion–extension motions, without damaging the facet joints. The question of whether low magnitudes of AT in addition to repetitive combined loading impacts the failure mechanics remains. Researchers have speculated that three axes of combined loading could increase the vulnerability of the IVD to injury (Ahmed et al., 1990; Pearcy and Hindle, 1991), and that such complex modes of loading more closely mimics loading in vivo (Pearcy and Tibrewal, 1984). Yet, three axes of combined loading, repetitive or acute, have rarely been investigated. A repetitive loading example was conducted by Gordon et al. (1991) who herniated all 14 tested functional spinal units (FSU) with the application of two static positions (7° flexion and >3° axial twist) combined with repetitive compression (1334 N), to an average of 40 000 loading cycles. Haberl et al. (2004) loaded specimens three times (30 s duration) with combinations of 200 N of compression, and up to 6 N m of flexion or extension, and 12.5 N m of static AT, and tracked the resulting kinematics, but did not report injury data. The mechanism of how chronic exposure to AT contributes to intervertebral joint failure mechanics remains poorly understood. The purpose of this study was to investigate the role of static AT, coupled with highly repetitive flexion–extension motions and static compression, on FSU failure mechanics. It was hypothesized that the addition of AT would not effect the onset, mode, or characteristics of specimen failure.

2. Methods

2.1. Specimen preparation

Eighteen C3–C4 porcine cervical motion segments were obtained from a common source to control for physical activity, diet, and age prior to death. Ideally, human lumbar specimens would be used in this study, but suitable human specimens are scarce and difficult to obtain. Given the functional, geometrical, and anatomical similarities between porcine cervical and human lumbar FSUs, porcine specimens were used as a model of human tissues in this study of injury mechanics (Oxland et al., 1991; Yingling et al., 1999). The porcine specimens were prepared, mounted and loaded (1472 N compression) as described in Callaghan and McGill (2001). Briefly, the specimens were thawed, dissected to osteo-ligamentous FSUs, and fixed into custom aluminum cups using wire looped around the laminae and anterior processes, screws into the vertebral bodies, and embedded in dental plaster. The specimens were wrapped with saline soaked plastic-backed cloth and plastic wrap to ensure continuous hydration. Approximately 0.7 cm^3 of barium sulfate radio-opaque mixed with blue dye (Coomassie Brilliant Blue G-mix: 0.25% dye, 2.5%MeOH, 97.25% distilled water) was injected into the IVD prior to testing. This solution has proved effective for permitting the documentation of nuclear material tracking using radiography (Callaghan and McGill, 2001). The 1472 N compressive load used in this study is approximately 14–22% of the average compressive strength of porcine cervical specimens reported in the literature. Aultman et al. (2004) and Gunning et al. (2001) found the average compressive strength of C3/4 and C5/6 specimens to be between approximately

Table 1
Average (±1 SD) intervertebral disc cross sectional area, preload creep, and maximum/minimum flexion–extension torque and angle values from the first RoM test, for the two test groups

Measure		Axial torque Mean (SD)	No axial torque Mean (SD)
Intervertebral disc cross sectional area (mm^2)		7.8 (0.7)	7.6 (0.9)
Preload creep (mm)		−0.96 (0.29)	−0.71 (0.29)
Maximum/minimum torque from first RoM test (N m)	Max.	26.8 (4.9)	26.8 (4.7)
	Min.	−8.9 (4.0)	−11.6 (4.7)
Maximum/minimum angle from first RoM test (°)	Max.	20.97 (2.26)	21.59 (3.12)
	Min.	−3.33 (1.68)	−3.33 (1.68)

6.5 kN and 10.6 kN. Parkinson et al. (in press) found no difference between C3/4 and C5/6 specimens, with average compressive strength values of 10.4 kN and 10.5 kN respectively. This magnitude of compression was chosen based on previous work that demonstrated 1472 N of compression when combined with repetitive flexion–extension motions reliably produced herniations after 6000 cycles (Callaghan and McGill, 2001). The specimens were randomly assigned to a testing group prior to mechanical loading. Based on the similarity in IVD cross sectional area ($P = 0.5395$), and conditioning test behaviour (Table 1), the two testing groups were deemed to be homogeneous.

2.2. Loading protocol

Prior to testing, each FSU was preloaded with 300 N of compressive force in a servo-hydraulic dynamic testing system (Model 8511, Instron Canada, Burlington, ON, Canada) for 15 min. The servomotor that produced the flexion–extension torques was set to a zero moment during the preload session. The end value represented an elastic equilibrium point of the specimen and was taken as the zero position for the remainder of testing. This position is within the neutral zone defined by Panjabi et al. (1989) and is consistent with the methods of Callaghan and McGill (2001). The FSU was then axial loaded with 1472 N of compressive force. The specimen was flexed and extended beyond the neutral zone five times during each range of motion (RoM) test at a rate of 0.5°/s. The angular values used for the subsequent dynamic test were selected from the last three moment-angle profile repeats from the RoM test. The angular positions were identified as the points (marking the boundary of the elastic zone) just before the torque versus angular position curve deviated from the linear section during both the flexion (rise) and extension (return) to the zero load position. This is similar to the boundary of the elastic zone as described by Panjabi et al. (1989), and the linear region identified by Adams et al. (1980). The torque at these positions (maximum flexion and extension angles) served as the torque targets for the RoM tests and the angular positions were used as targets for the dynamic repetitive tests. Three dimensional RoM was assessed through the application of moments to the unloaded FSU and a pre-test X-ray was taken.

To ensure repeatability of positioning in subsequent manual tests, the position of the specimen (top cup versus bottom cup) in the first manual test was measured using a goniometer in each axis sequentially. A ±3 N m torque (Digital Torque Gauge DTGHS, Chatillon Force Measurement, Digital Measurement Metrology, Brampton, Ontario, Canada) was applied to the unloaded FSU about the flexion–extension, lateral bend, and axial twist axes while the resulting angular motion was recorded using a potentiometer (Model 6639S-001-502, resistance 5 KΩ ± 15%, linearity ± 2.0%, Bourns, Electrosonic, Mississauga, ON, Canada) attached between the bottom

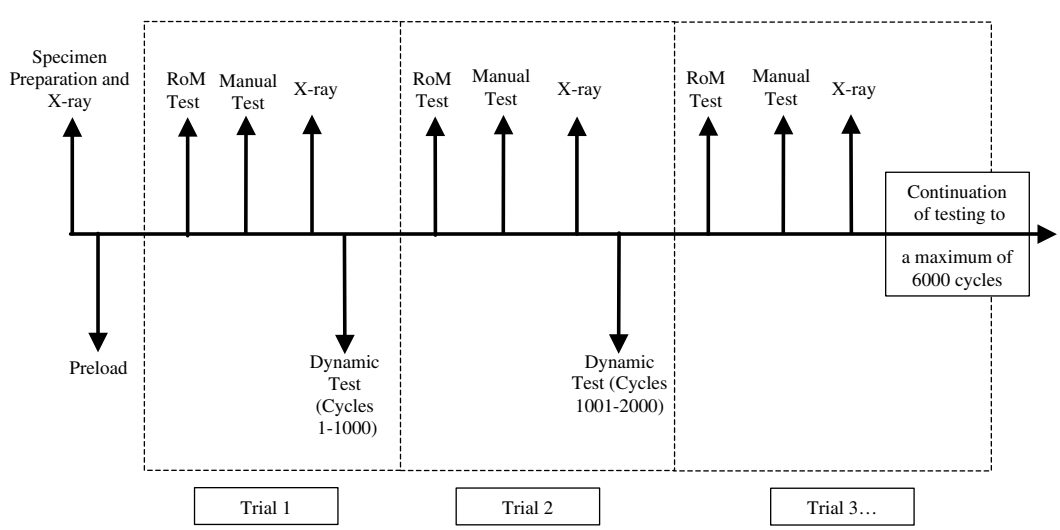

Fig. 1. The testing protocol timeline with the testing repeats up to a maximum of 6000 cycles.

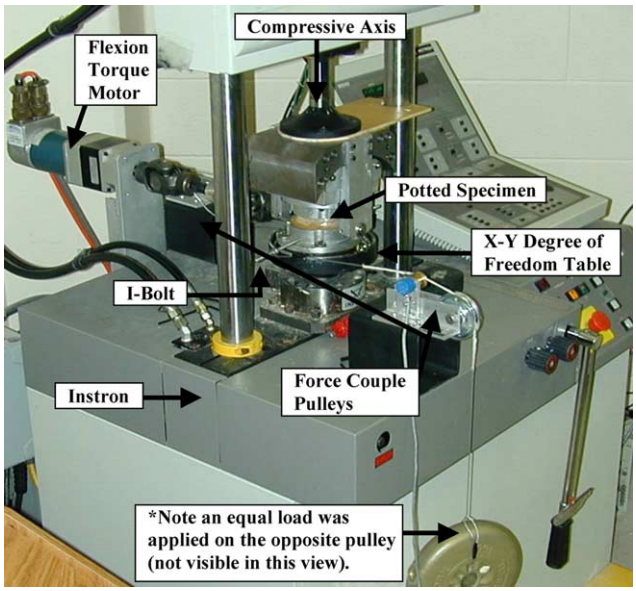

Fig. 2. The servo-hydraulic dynamic testing system applying axial compression (Instron), flexion–extension motions (servomotor), and axial torque to a specimen via a force couple (created by hanging equal masses off pulleys on opposite sides of the specimen). The potted specimen mounting cup sat on a ball bearing table which allowed unconstrained X–Y motion and axial rotation.

and top specimen cups. Both the potentiometer and torque transducer were A/D converted at 64 samples/s.

The FSUs were then tested to 1000 cycles of repetitive flexion–extension motions with static compressive force and with or without AT (through random assignment). Repeats of the tests and 1000 cycles of exposure, representing one trial as depicted in Fig. 1, were continued to a maximum of 6000 cycles or until the testing of the FSU became compromised (bottom cup contacted X–Y translation table or if the top and bottom cup contacted) by the instrumentation (Fig. 2). To create the 5 N m AT moment applied in the AT condition, weighted cables were attached perpendicularly to two I-bolts set in the bottom cup to produce a force couple (Fig. 2). A second potentiometer was attached to the front pulley to measure any rotational angular deformation during the dynamic testing. The specimens were cyclically loaded at a rate of 1 Hz in angular positional control, with the total testing time averaging six hours per specimen. The flexion–extension angular position and torque, axial compressive force and axial deformation, and the rotational deformation were A/D converted at a rate of 30 Hz.

2.3. Post-loading protocol

Once testing was completed the specimen was removed from the cups and X-rays were taken of the intact and sectioned (through the disc) specimen. The condition of the specimen was inspected for fractures and posterior accumulation of the dye stained nucleus pulposus material was photographed and recorded. The facets were manually tested for resistance to pressure and visually inspected, and confirmation of fracture was achieved radiographically. Data on the damage to the cartilage on the articular surfaces of the facets was not included since the cartilage could have been damaged during the post-testing dissection procedures.

The X-rays were blinded once all of the specimens were tested, and were read by a radiographic expert from the Ontario Veterinary College (University of Guelph, Guelph, ON, Canada). Using the radiographic criteria from Callaghan and McGill (2001), the trial in which the presence of herniation was observed was recorded. Nuclear extrusion and annular bulge were both described as herniation since they can not always be distinguished radiographically (Adams and Hutton, 1982).

2.4. Data reduction

Axial creep (mm) from the dynamic tests was selected for every test cycle when the specimen crossed the zero position. Flexion–extension axis stiffness (N m/degree) and hysteresis (N m degree) values from the RoM test were calculated using the torque and angle values from the last three repeats. Load–displacement curves have been shown to become consistent following two repeats (Dhillon et al., 2001). An average stiffness was calculated from the slope of the line connecting the maximum and minimum torque and angle values (the ends of the linear region) for each of the last three repeats in the RoM test. These stiffness values were averaged across the last three repeats to provide the overall average stiffness for the specimen. The hysteresis energy values were calculated as the difference in the area between the loading and unloading curves. The area was calculated using the trapezoidal integration method. The angle and torque data for the last ten cycles of each trial were averaged to calculate the dynamic flexion–extension axis stiffness values. From the manual tests, the range of angular deformation was normalized using the initial values. The creep due to the 5 N m of applied AT was measured at the zero position from the beginning to the end of dynamic testing.

2.5. Statistical analyses

Two-way ANOVAs for group (AT and no AT) and trial (repeated measure) were applied to the RoM, dynamic, and manual test data. For the IVD size, preload axial creep, and initial flexion–extension axis maximum/minimum torque and angular values from the RoM test, t-tests for two-samples were applied. For the two groups (with and without AT) a test for equality of the binomial proportion was used to analyse the occurrence of herniation, and the Fisher's exact test was used for the

number of endplate fractures and facet fractures. The α-value was set to 0.05 for all tests.

3. Results

The occurrence of facet fractures was found to be significantly higher ($P = 0.028$) in the AT group which had 7/9 specimens with at least one facet fracture, compared to the 2/9 facet fractures in the no AT group. The C4 compression facet failed for all AT specimens that had a facet fracture. Whereas only one FSU in the no AT group had the C4 compression facet fail. Results of the macroscopic inspection revealed delamination of the annulus in all of the specimens, regardless of test group. There was no difference ($P = 0.833$) in the number of endplate fractures or herniations after 6000 cycles of loading (both 7/9) between the two groups. Statistically more ($P = 0.049$) specimens in the AT group herniated (71%) than the no AT group (29%) at the 3000 cycles limit established by the hysteresis energy and stiffness responses. The plots of the trial compared to the initiation of annular track formation (Fig. 3A) and herniation (Fig. 3B) demonstrate that the failure events occurred earlier in the AT group specimens.

A significant ($P < 0.0001$) trial effect was found for the maximum and minimum angle the specimen reached during the RoM test, but there was no significant group or interaction effects for these RoM test angles. The maximum and minimum angle decreased in magnitude for the same torque as the trial number increased (i.e. the specimens became more stiff). However, interaction effects were found for the RoM test flexion–extension axis hysteresis energy ($P = 0.018$) and cycle stiffness ($P = 0.024$). The two groups behaved differently as the number of cycles (trial number) increased. Examining the interaction patterns revealed that the AT group showed a significant increase in the hysteresis energy after 1000–3000 ($P < 0.014$) cycles whereas the no AT group returned to near original hysteresis values before continuing to decrease (Fig. 4). For stiffness, the two groups were not different until 4000 cycles ($P = 0.016$), where the no AT group plateaued and the AT group stiffness continued to increase (Fig. 5). During the RoM tests, the maximum applied flexion/extension angles and moments were 18.5° (SD 2.3)/−1.3° (SD 0.7) and 26.9 N m (SD 4.1)/−12.2 N m (SD 3.9) for the axial torque group and were 19.1° (SD 3.1)/−1.3° (SD 0.9) and 29.2 N m (SD 4.5)/−12.9 N m (SD 4.7) for the no-axial torque group. There was no statistical difference between the flexion or extension angles and moments applied in the two loading groups ($P > 0.152$).

There were no significantly different responses for axial creep during the dynamic tests ($P > 0.140$). Trial effects were found to be significant ($P < 0.0001$) for the flexion–extension axis cycle stiffness and for the range of torque applied. All of these values increased with increasing trial number. There were no group or interaction effects for stiffness ($P = 0.751, 0.984$) or range of torque ($P = 0.593, 0.901$). The FSU experienced creep due to the application of 5 N m AT resulting in an average new moment of 4.98 N m (SD 0.01) and 3.37° (SD

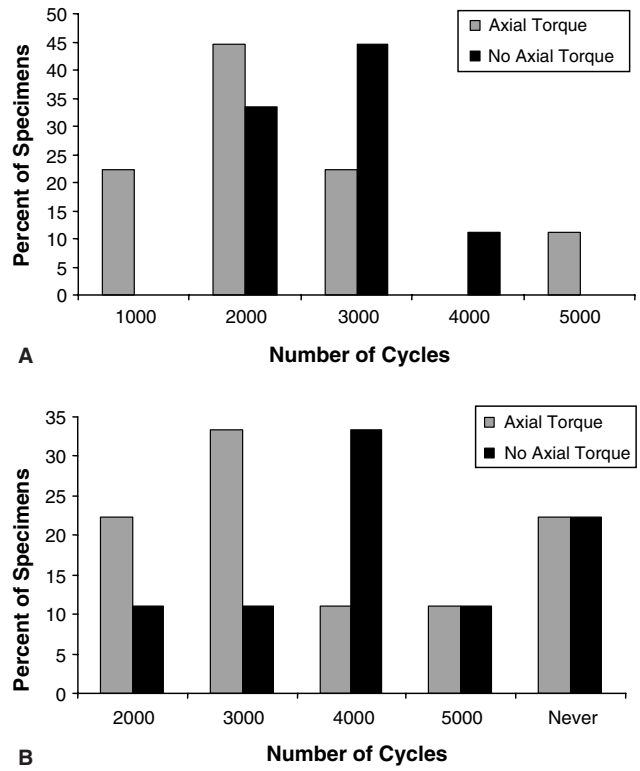

Fig. 3. The distribution, per 1000 cycles, of track initiation (A) and herniation (B) of nuclear material through the annulus of the intervertebral disc as determined from planar radiographs.

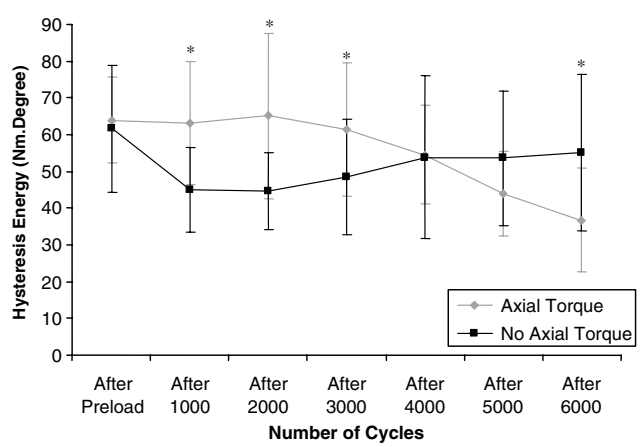

Fig. 4. The average hysteresis energy changes and ±1 standard deviation about the flexion–extension axis during the RoM test for each loading condition. Statistical differences are indicated with asterisks (*).

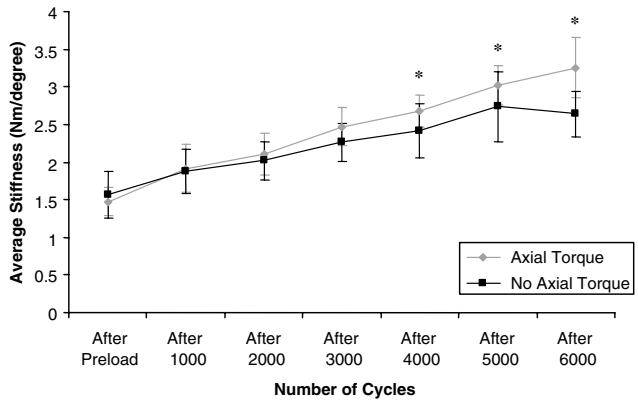

Fig. 5. Average angular flexion–extension axis stiffness and ±1 standard deviation for the RoM tests. Statistical differences are indicated with asterisks (*).

1.66) total creep by the end of dynamic testing due to the constraints of the jig.

The angular deformation recorded from the unloaded specimens in six directions, flexion–extension, right/left lateral bend, and clockwise and counterclockwise axial twist was not significantly different between the two groups and there were no significant interactions between group and trial. However, there was a significant trial effect for each of the paired movements, with $P = 0.0002$ for flexion–extension motions and $P < 0.0001$ for both lateral bend and axial twist motions. The angular deformation for all measures increased with increasing cycle number. During the flexion–extension and lateral bend motions, the average angular deformation recorded for no AT group tended to overlay or slightly exceed the AT group values. The trend for axial twist was the opposite with the average angular deformation of the AT group exceeding the no AT group for each trial.

4. Discussion

Static AT increased the vulnerability of FSU in repetitive combined loading by changing the failure mechanism. Specifically, the addition of 5 N m of static AT appears to result in an earlier onset of herniation, higher incidence of facet fracture, and higher energy dissipation and specimen stiffness up to approximately 3000 cycles of loading. These findings suggest AT coupled with combined loading accelerates the FSU failure. From this investigation it appears that the failure of the facet and IVD are not necessarily independent, and so any damage leads to an accelerated destruction of both structures.

While all specimens ultimately herniated in this study, the addition of AT, at the levels of loading tested, did contribute to earlier initiation of disc herniation. The IVD is strongest at bearing compressive loads, but is not well suited to resist combined flexion and axial rotation, which generate tensile stresses resisted only by the annulus fibrosus in the IVD (Adams and Dolan, 1995; Green et al., 1993; Panjabi et al., 1984; Pearcy, 1993). In addition to an increase in flexion–extension moment applied when the facets contact (Haberl et al., 2004), the IVD is required to resist more tension when exposed to AT in midranges of flexion due to the increased initial spacing between the facet joints (Pearcy, 1993; Pearcy and Hindle, 1991). As the facets begin to fail the FSU is able to rotate further, which again increases the tensile strain on the annulus, contributing to IVD damage. At the end of testing the AT group specimens had an average creep of approximately three degrees, which has been reported as the amount of rotation where facets fail (Adams and Hutton, 1981). This postulated failure mechanism is supported by the higher hysteresis energy loss (Fig. 4) and cycle stiffness (Fig. 5), earlier herniation onset, higher facet fractures, as well as the increased axial rotation trends in the manual RoM test, observed in the AT group.

As in any in vitro study using an animal model in place of human tissue, there were limitations that define the context of the work. The use of an animal model provides a homogeneous specimen population and control over variables such as age, diet, weight, level of physical activity, and disc degeneration, but limits the direct applicability of the results to humans. The human lumbar spine supports large compressive forces due to the weight of the upper body and head. The loading experienced by pig cervical vertebrae is also highly compressive given the need to support a cantilevered head (Yingling et al., 1999). Yingling et al. (1999) found porcine cervical vertebrae resembled human lumbar vertebrae geometrically and functionally, while Oxland et al. (1991) found anatomical similarities. Of particular interest, Yingling et al. (1999) found that the facet angle is closer in cervical porcine to human lumbar vertebrae than porcine lumbar specimens. The in vitro porcine model used consisted of only specimens with no disc degeneration (i.e. Grade 1) as defined by Galante (1967). It is well established that Grade 1 specimens herniate more readily than degenerated IVD, but less readily than the slightly degenerated lower lumbar disc of people aged between 40 and 50 (Adams and Hutton, 1982). Likewise, the use of Grade 1 specimens may introduce a 'margin of error' with respect to injury formation. Freezing of tissue has not been shown to change the compressive elastic properties of the porcine IVD (Callaghan and McGill, 1995), or alter the time-dependent behaviour of the human IVD (Dhillon et al., 2001). Further, Adams and Dolan (1996) mentioned that post mortem changes are small with respect to the variability inherent in human specimens. The primary difference between loading living and dead tissue is that in vivo there is an inflammatory response; a feedback based system leading to recovery periods (sleep/rest). However, in

poorly vascularized tissues the cell-mediated repair processes are not necessarily inflammatory. Further, the physiological repair mechanisms of microfractures in bone (Brinckmann et al., 1988), and synthesis of proteoglycans (Urban et al., 1978) and collagen (Adams and Hutton, 1982), take much longer than two weeks (several weeks to >1 year). Therefore, the 6000 cycles of loading used as the maximum in this study, could be easily accumulated in vivo in shorter time periods than required for the repair processes to occur. The testing conditions were limited to examining compressive load with dynamic flexion–extension motions of FSUs and one direction static axial twist, whereas the spine moves with six degrees of freedom.

The increase in stiffness found in this study for the AT group up to 4000 cycles illustrates the increased FSU damage sustained by this group. Thompson et al. (2000) found an increase in stiffness with an increase in damage of the IVD. Callaghan and McGill (2001) and Yoganandan et al. (1994) also found an increase in stiffness with increase in exposure time during repeated combined loading. However, the three axes combined loading study by Gordon et al. (1991) showed no correlation between damage and biomechanical parameters (stiffness or hysteresis), and no differences prior to or following injury. Comparison of these repetitive loading results with the acute loading study by Aultman et al. (2004), demonstrate that the mechanism of failure is dependent on the type of loading. Aultman et al. (2004) found that AT decreased the FSU's ultimate compressive strength and caused endplate fractures but no damage to facets. The high percentage of specimen herniation in the no AT group is consistent with the findings of Callaghan and McGill (2001).

The low level of applied static AT (5 N m) accelerated IVD and facet fracture when combined with compression and flexion–extension motions. Adams et al. (2002) postulated that in vivo the maximum AT carried by a lumbar spine joint is 6–12 N m. The prevalence of painful facets was as high as 15% in a working population (Schwarzer et al., 1994), and pain due to disruption of the internal structure of the disc was 40% in a low back pain population (Schwarzer et al., 1995a). Given the prevalence and risks attributed to this type of loading, scenarios that combine axial AT exposure with repetitive motions need to be assessed in order to prevent the risks of spine injuries or low back pain. These findings suggest further study of AT in combined loading, as well as the establishment of an exposure guideline for this type of repetitive loading is warranted.

5. Conclusions

While AT has been reported to be insufficient to contribute to the failure of the IVD (Adams and Hutton, 1981; Pearcy and Hindle, 1991), three axes of combined loading (highly repetitive flexion–extension motion, static compression, and static AT) appeared to damage both the IVD and facets. The ability of small magnitudes of static AT to alter the failure mechanics of the intervertebral disc and vertebrae in combined loading paradigms indicate the complexity of the relationship amongst three axes of loading and the FSU structures.

Acknowledgements

We would like to thank the Natural Science and Engineering Research Council of Canada for their financial support. Dr. Jack P. Callaghan is supported by a Canada Research Chair in Spine Biomechanics and Injury Prevention. Janessa Drake is supported by a Canadian Institute for the Relief of Pain and Disability (CIRPD)/Canadian Institutes of Health Research (CIHR) Doctoral Research Award.

We would also like to thank Dr. Dobson for his radiography advice, University of Waterloo Statistical Consulting Service, and Jeff Rice, Wendell Prime, and Chris Birker for their technical assistance.

References

Adams, M.A., Dolan, P., 1995. Recent advances in lumbar spinal mechanics and their clinical significance. Clin. Biomech. 10, 3–19.

Adams, M.A., Dolan, P., 1996. Time-dependent changes in the lumbar spine's resistance to bending. Clin. Biomech. 11, 194–200.

Adams, M.A., Hutton, W.C., 1981. The relevance of torsion to the mechanical derangement of the lumbar spine. Spine 6, 241–248.

Adams, M.A., Hutton, W.C., 1982. Prolapsed intervertebral disc: a hyperflexion injury. Spine 7, 184–191.

Adams, M.A., Bogduk, N., Burton, K., Dolan, P., 2002. The Biomechanics of Back Pain. Churchill Livingstone, Toronto.

Adams, M.A., Hutton, W.C., Stott, J.R.R., 1980. The resistance to flexion of the lumbar intervertebral joint. Spine 5, 245–253.

Ahmed, A.M., Duncan, N.A., Burke, N.A., 1990. The effect of facet geometry on the axial torque-rotation response of lumbar motion segments. Spine 15, 391–401.

Aultman, C.D., Drake, J.D.M., Callaghan, J.P., McGill, S.M., 2004. The effect of static torsion on the compressive strength of the spine: an in vitro analysis using a porcine spine model. Spine 29, E304–E309.

Boden, S.D., Davis, D.O., Dina, T.S., Patronas, N.J., Wiesel, S.W., 1990. Abnormal magnetic-resonance scans of the lumbar spine in asymptomatic subjects. A prospective investigation. J. Bone Joint Surg. 72-A, 403–408.

Boos, N., Semmer, N., Elfering, A., Schade, V., Gal, I., Zanetti, M., Kissling, R., Buchegger, N., Hodler, J., Main, C.J., 2000. Natural history of individuals with asymptomatic disc abnormalities in magnetic resonance imaging: predictors of low back pain-related medical consultation and work incapacity. Spine 25, 1484–1492.

Brinckmann, P., Biggemann, M., Hilweg, D., 1988. Fatigue fracture of human lumbar vertebrae. Clin. Biomech. 21, 425–433.

Callaghan, J.P., McGill, S.M., 1995. Frozen storage increases the ultimate compressive load of porcine vertebrae. J. Orthop. Res. 13, 809–812.

Callaghan, J.P., McGill, S.M., 2001. IVD herniation: studies on a porcine model exposed to highly repetitive flexion/extension motion with compressive force. Clin. Biomech. 16, 28–37.

Dhillon, N., Bass, E.C., Lotz, J.C., 2001. Effect of frozen storage on the creep behavior of human intervertebral discs. Spine 26, 883–888.

Farfan, H.F., 1969. Effects of torsion on the intervertebral joints. Can. J. Surg. 12, 336–341.

Farfan, H.F., 1970. The effect of torsion on lumbar intervertebral joints: the role of torsion in the production of disc degeneration. J. Bone. Joint Surg. Am. 52A, 468–497.

Galante, J.O., 1967. Tensile properties of the human lumbar annulus fibrosus. Acta. Orthop. Scand. Suppl. 100, 5–91.

Gordon, S.J., Yang, K.H., Mayer, P.J., Mace Jr., A.H., Kish, V.L., Radin, E.L., 1991. Mechanism of disc rupture—a preliminary report. Spine 16, 450–456.

Green, T.P., Adams, M.A., Dolan, P., 1993. Tensile properties of the annulus fibrosus. II. Ultimate tensile strength and fatigue life. Eur. Spine. J. 2, 209–214.

Gunning, J.L., Callaghan, J.P., McGill, S.M., 2001. Spinal posture and prior loading history modulate compressive strength and type of failure in the spine: a biomechanical study using a porcine cervical spine model. Clin. Biomech. 16, 471–480.

Haberl, H., Cripton, P.A., Orr, T.E., Beutler, T., Frei, H., Lanksch, W.R., Nolte, L.P., 2004. Kinematic response of lumbar functional spinal units to axial torsion with and without superimposed compression and flexion/extension. Eur. Spine. J. 13, 560–566.

Ito, M., Incorvaia, K.M., Yu, S.F., Fredrickson, B.E., Yuan, H.A., Rosenbaum, A.E., 1998. Predictive signs of discogenic lumbar pain on magnetic resonance imaging with discography correlation. Spine 23, 1252–1258.

Jager, M., Jordan, C., Luttmann, A., Laurig, W., 2000. Evaluation and assessment of lumbar load during total shifts for occupational manual materials handling jobs within the Dortmund Lumbar Load Study—DOLLY. Int. J. Ind. Ergon. 25, 553–571.

Jensen, M.C., Brant-Zawadski, M.N., Obuchowski, N., Modic, M.T., Malkasian, D., Ross, J.S., 1994. Magnetic resonance imaging of the lumbar spine in people without back pain. N. Engl. J. Med. 331, 69–73.

Kelsey, J.L., Githens, P.B., White 3rd, A.A., Holford, T.R., Walter, S.D., O'Connor, T., Ostfeld, A.M., Weil, U., Southwick, W.O., Calogero, J.A., 1984. An epidemiologic study of lifting and twisting on the job and risk for acute prolapsed lumbar intervertebral disc. J. Orthop. Res. 2, 61–66.

Krismer, M., Haid, C., Rabl, W., 1996. The contribution of anulus fibers to torque resistance. Spine 21, 2551–2557.

Kumar, S., 1990. Cumulative load as a risk factor for back pain. Spine 15, 1311–1316.

Marras, W.S., Lavender, S.A., Leurgans, S.E., Rajulu, S.L., Allread, W.G., Fathallah, F.A., Ferguson, S.A., 1993. The role of dynamic three-dimensional trunk motion in occupationally-related low back disorders: the effects of workplace factors, trunk position and trunk motion characteristics on risk of injury. Spine 18, 617–628.

McCall, I.W., Park, W.M., O'Brien, J.P., 1979. Induced pain referral from posterior lumbar elements in normal subjects. Spine 4, 441–446.

Norman, R., Wells, R., Neumann, P., Frank, J., Shannon, H., Kerr, M., 1998. A comparison of peak vs cumulative physical work exposure risk factors for the reporting of low back pain in the automotive industry. Clin. Biomech. 13, 561–573.

Oxland, T.R., Panjabi, M.M., Southern, E.P., Duranceau, J.S., 1991. An anatomic basis for spinal instability: a porcine trauma model. J. Orthop. Res. 9, 452–462.

Panjabi, M.M., Duranceau, J.S., Oxland, T.R., Bowen, C.E., 1989. Multidirectional instabilities of traumatic cervical spine injuries in a porcine model. Spine 14, 1111–1115.

Panjabi, M.M., Krag, M.H., Chung, T.Q., 1984. Effects of disc injury on mechanical behaviour of the human spine. Spine 9, 707–713.

Parkinson, R.J., Durkin, J.L., Callaghan, J.P., in press. Estimating the compressive strength of the porcine cervical spine: an examination of the utility of DXA. Spine.

Pearcy, M.J., 1993. Twisting mobility of the human back in flexed postures. Spine 18, 114–119.

Pearcy, M.J., Hindle, R.J., 1991. Axial rotation of lumbar intervertebral joints in forward flexion. Proc. Inst. Mech. Eng. [H]. 205, 205–209.

Pearcy, M.J., Tibrewal, S.B., 1984. Axial rotation and lateral bending in the normal lumbar spine measured by three-dimensional radiography. Spine 9, 582–587.

Punnet, L., Fine, L.J., Keyserling, W.M., Herrin, G.D., Chaffin, D.B., 1991. Back disorders and nonneutral trunk postures of automobile assembly workers. Scand. J. Work. Environ. Health. 17, 337–346.

Schwarzer, A.C., Aprill, C.N., Derby, R., Fortin, J., Kine, G., Bogduk, N., 1994. Clinical features of patients with pain stemming from the lumbar zygapophysial joints. Is the lumbar facet syndrome a clinical entity? Spine 19, 1132–1137.

Schwarzer, A.C., Aprill, C.N., Derby, R., Fortin, J., Kine, G., Bogduk, N., 1995a. The prevalence and clinical features of internal disc disruption in patients with chronic low back pain. Spine 20, 1878–1883.

Schwarzer, A.C., Wang, S.C., O'Driscoll, D., Harrington, T., Bogduk, N., Laurent, R., 1995b. The ability of computed tomography to identify a painful zygapophysial joint in patients with chronic low back pain. Spine 20, 907–912.

Thompson, R.E., Pearcy, M.J., Downing, K.J.W., Manthey, B.A., Parkinson, I.H., Fazzalari, N.L., 2000. Disc lesions and the mechanics of the intervertebral joint complex. Spine 25, 3026–3035.

Urban, J.P.G., Holm, S., Maroudas, A., 1978. Diffusion of small solutes into the intervertebral disc. An in vivo study. Biorheology 15, 203–223.

Yingling, V.R., Callaghan, J.P., McGill, S.M., 1999. The porcine cervical spine as a model of the human lumbar spine: an anatomical, geometric, and functional comparison. J. Spinal. Disord. 12, 415–423.

Yoganandan, N., Cusick, J.F., Pintar, F.A., Droese, K., Reinartz, J., 1994. Cyclic compression–flexion loading of the human lumbar spine. Spine 19, 784–790.